

# Bulk Waves in the Infinite Electric-Magnetic-Elastic Plate with Mixed Boundary Conditions

Genquan Xie<sup>1\*</sup>, Xingpeng Song<sup>1</sup>, Xiaodong Xiao<sup>2</sup>

<sup>1</sup>Civil Engineering School, Hunan University of Science and Technology, Xiangtan, China

<sup>2</sup>Experimental School Affiliated to Loudi No. 1 Middle School, Loudi, China

Email: \*xiaoyuanyixiong@163.com

**How to cite this paper:** Xie, G.Q., Song, X.P. and Xiao, X.D. (2021) Bulk Waves in the Infinite Electric-Magnetic-Elastic Plate with Mixed Boundary Conditions. *Journal of Electromagnetic Analysis and Applications*, 13, 21-39.

<https://doi.org/10.4236/jemaa.2021.132002>

**Received:** February 17, 2021

**Accepted:** February 25, 2021

**Published:** February 28, 2021

Copyright © 2021 by author(s) and Scientific Research Publishing Inc. This work is licensed under the Creative Commons Attribution International License (CC BY 4.0).

<http://creativecommons.org/licenses/by/4.0/>



Open Access

---

## Abstract

A dynamic solution is presented for the propagation of waves in an electric-magneto-elastic plate composed of piezoelectric, piezomagnetic materials and elastic matrix. The electric-magneto-elastic plate is polarized along the thickness direction. The generalized displacements are expressed as the sum of the gradient of a scalar (dilatation wave) and the curl of a vector (shear wave). With the help of dynamic equilibrium equations and geometric equations, we can obtain dynamic equations of the dilatation wave and the shear wave. The conclusion that the types of the dilatation waves and the shear waves remain unchanged after being reflected by the boundary can be obtained through the analysis of these kinetic equations. The dispersion properties and phase velocity surface of the dilatation and shear wave can be obtained by solutions of dynamic equilibrium equations. Influences of the piezoelectric and piezomagnetic parameters on wave characteristics are discussed.

## Keywords

Bulk Wave, Electric-Magneto-Elastic Plate, Dilatation Wave, Shear Wave, Dispersion Properties, Phase Velocity Surface

---

## 1. Introduction

The electric-magneto-elastic structures or materials have the capacity of converting energy from one form to the other (among mechanical, magnetic and electric energy) [1] [2], and show good application prospects in smart sensors, actuators, transducers and many other emerging devices. There is a strong need

for theories or techniques that can predict the coupled response of these smart materials, as well as structures made up of them. Static and dynamic characteristics of plates as well as infinite cylinder have been studied in the literature. Piotr Cupiał [3] discussed a perturbation solution of the natural frequencies and mode shapes of a piezoelectric rectangular plate modeled as a three-dimensional body. Guoquan Nie *et al.* [4] instigated shear horizontal (SH) waves propagating in piezoelectric-piezomagnetic bilayer system with an imperfect interface. Hamdi Ezzin *et al.* [5] presented a dynamic solution for the propagation of harmonic waves in magneto-electro-elastic plates composed of piezoelectric BaTiO<sub>3</sub>(B) and magnetostrictive CoFe<sub>2</sub>O<sub>4</sub>(F) material. Xiao Guo *et al.* [6] dealt with effects of functionally graded interlayers on dispersion relations of shear horizontal waves in layered piezoelectric/piezomagnetic cylinders. J.G. Yu *et al.* [7] proposed a double orthogonal polynomial series approach to solving the wave propagation problem in a two-dimensional (2-D) structure. Yu Pang *et al.* [8] employed the stiffness matrix method and the transfer matrix method to investigate SH bulk/surface waves propagating in the corresponding infinite/semi-infinite piezoelectric (PE)/piezomagnetic (PM) and PM/PE periodically layered composites. Feng-Ming Li *et al.* [9] investigated the elastic wave propagation in phononic crystals with piezoelectric and piezomagnetic inclusions. Wei and Li [10] investigated the direction dependence of surface wave speed and the influence of electrically and magnetically short/open circuit conditions. Yu Pang *et al.* [11] analyzed the reflection and refraction of a plane wave incidence obliquely at the interface between piezoelectric and piezomagnetic media. M. Arfi [12] used non-local elasticity to analyze waves in a functionally graded magneto-electro-elastic nano-rod.

The above existing works of literature are mainly researches on surface waves in electric-magneto-elastic plates. Hence in the present study, characteristics of bulk wave in an electric-magneto-elastic plate have been studied, the physical of waves and the geometric dispersion of waves along the thickness of an infinite plate are simultaneously studied. The elastic displacement is expressed as the sum of a scalar gradient and a vector curl. Based on dynamic equilibrium equations and geometric equation, we can obtain dynamic equations of the dilatation wave and shear wave, and the dispersion properties and phase velocity surface of the dilatation and shear wave can be obtained by solutions of dynamic equilibrium equations. The main aim of the study is to evaluate the influence of piezoelectric, piezomagnetic and elastic parameters on characteristics of bulk wave in an electric-magneto-elastic plate.

## 2. Formulation

The electric-magneto-elastic material possess characteristic of the magnetic-electric-mechanical coupling. In this paper, only wave of magnetic potential and electric one and displacements are considered, so that the displacement vector  $\mathbf{u}$ , electric potential  $\phi$ , and magnetic potential  $\psi$  are chosen as basic

variables. The basic equations are listed as follows.

The constitutive equations of the electric-magneto-elastic material are given by

$$\sigma_{ij} = C_{ijkl} \varepsilon_{kl} - e_{ijn} E_n - q_{ijn} H_n \quad (1)$$

$$D_n = e_{kln} \varepsilon_{kl} + g_{mn} E_m + \alpha_{mn} H_m \quad (2)$$

$$B_n = q_{kln} \varepsilon_{kl} + \alpha_{mn} E_m + \mu_{mn} H_m \quad (3)$$

where  $\sigma_{ij}$ ,  $\varepsilon_{kl}$ ,  $D_m$  and  $B_m$  are, respectively, stresses, strains, electric displacements and magnetic induction tensors,  $C_{ijkl}$  are the elastic constants,  $e_{ijn}$  the piezoelectric tensors,  $g_{mn}$  the dielectric tensors,  $\alpha_{mn}$  the magnetic-electric mutual inductance tensors,  $q_{ijn}$  the piezomagnetic tensors,  $\mu_{mn}$  the magnetic permeability tensors, all the subscripts  $i, j, k, l, m, n = 1, 2, 3$ , two identical subscripts in an integral expression denote the sum of Einstein.

The generalized dynamic equilibrium equations absent of the mechanical body force are given by

$$\sigma_{ij,j} = \rho \ddot{u}_i \quad (4)$$

$$D_{n,n} = 0 \quad (5)$$

$$B_{n,n} = 0 \quad (6)$$

where  $\rho$  the mass density, the comma in subscript indicates partial derivative.

The generalized geometrical equations are

$$\varepsilon_{kl} = \frac{1}{2} (u_{k,l} + u_{l,k}) \quad (7)$$

$$E_m = -\varphi_{,m} \quad (8)$$

$$H_m = -\psi_{,m} \quad (9)$$

Combing of Equations (1)-(9), one easily obtains

$$\frac{1}{2} C_{ijkl} (u_{k,lj} + u_{l,kj}) - e_{ijn} \varphi_{,nj} - q_{ijn} \psi_{,nj} = \rho \ddot{u}_i \quad (10a)$$

$$\frac{1}{2} e_{kln} (u_{k,ln} + u_{l,kn}) + g_{mn} \varphi_{,mn} + \alpha_{mn} \psi_{,mn} = 0 \quad (10b)$$

$$\frac{1}{2} q_{kln} (u_{k,ln} + u_{l,kn}) + \alpha_{mn} \varphi_{,mn} + \mu_{mn} \psi_{,mn} = 0 \quad (10c)$$

Let us consider an anisotropic electric-magneto-elastic plate as shown in **Figure 1**,  $x_1 0 x_2$  is the middle surface of the plate which is infinite in the two directions  $x_1$  and  $x_2$ ,  $x_3$  is the thickness direction.

The angle between the incident direction of the wave and the  $x_1$ -axis is assumed to be  $\theta$ , so that the following relationships can be obtained as

$$\left. \begin{aligned} k_1 &= k \cos \theta \\ k_2 &= k \sin \theta \end{aligned} \right\} \quad (11)$$

where  $k$  is wave number in the plane  $x_1 0 x_2$ .

The elastic wave tensor can be expressed as the following form

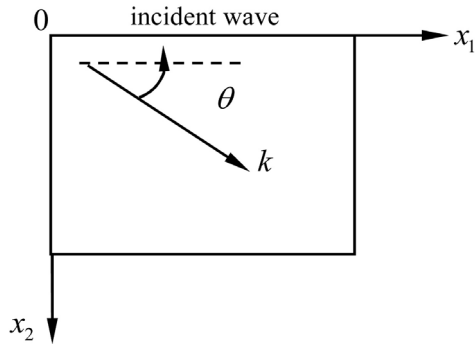


**Figure 1.** The model of electric-magnetic-elastic plate.

$$u_i = \Phi_{,i} + \varepsilon_{ijk} \Psi_{j,k} \tag{12}$$

where  $\varepsilon_{ijk}$  is a permutation tensor, the scalar field  $\Phi$  and the vector field  $\Psi_j$  are assumed to be

$$\Phi = f(x_3) e^{i(k_1 x_1 + k_2 x_2 - \omega t)} \tag{13}$$

$$\Psi_j = g_j(x_3) e^{i(k_1 x_1 + k_2 x_2 - \omega t)} \tag{14}$$

In Equation (13),  $f(x_3)$  is tried to take the following form

$$f(x_3) = A_m \sin(\eta_m^d x_3) \tag{15}$$

where  $\eta_m^d$  is the  $m$ th wave number of the dilatation wave in the thickness direction  $x_3$ .

In Equation (14),  $g_j(x_3)$  is tried to take the following form

$$g_j(x_3) = F_{jn} \sin(\eta_n^s x_3) \tag{16}$$

where  $\eta_m^s$  is the  $m$ th wave number of the shear wave in the thickness direction.

The electric-magneto-elastic plate is assumed to be polarized in the direction  $x_3$ , the static electric-potential and magneto-potential is tried to take the following forms

$$\varphi = \left[ f'_\varphi(x_3) + i(k_1 g_{2\varphi}(x_3) - k_2 g_{1\varphi}(x_3)) \right] e^{i(k_1 x_1 + k_2 x_2 - \omega t)} \tag{17}$$

$$\psi = \left[ f'_\psi(x_3) + i(k_1 g_{2\psi}(x_3) - k_2 g_{1\psi}(x_3)) \right] e^{i(k_1 x_1 + k_2 x_2 - \omega t)} \tag{18}$$

where

$$\begin{cases} f_\varphi(x_3) = A_m^\varphi \sin(\eta_m^d x_3) \\ f_\psi(x_3) = A_m^\psi \sin(\eta_m^d x_3) \end{cases} \tag{19}$$

$$\begin{cases} g_{j\varphi}(x_3) = F_{jn}^\varphi \sin(\eta_n^s x_3) \\ g_{j\psi}(x_3) = F_{jn}^\psi \sin(\eta_n^s x_3) \end{cases} \tag{20}$$

### 3. Numeric Example and Discussion

In the subsequent numeric example, the electric-magnetic-elastic plate is as-

sumed to be polarized in the direction  $x_3$ , the thickness of the plate is  $2h$ , the mass density  $\rho = 7454 \text{ kg/m}^3$ , the material parameters are given by **Tables 1-3**.

Except these parameters given by **Tables 1-3**, the others are assumed to be zeros.

### 3.1. Mixed Boundary Condition

For smooth rigid boundary conditions, namely,  $u_3|_{x_3=\pm h} = 0$ ,

$$\sigma_{23}|_{x_3=\pm h} = \sigma_{31}|_{x_3=\pm h} = 0, \quad \varphi|_{x_3=\pm h} = 0, \quad D_1|_{x_3=\pm h} = D_2|_{x_3=\pm h} = 0, \quad \psi|_{x_3=\pm h} = 0,$$

$B_1|_{x_3=\pm h} = B_2|_{x_3=\pm h} = 0$ ,  $\eta_m^d$  and  $\eta_m^s$  which satisfy the boundary condition are taken as the following forms

$$\eta_m^d = \frac{m\pi}{2h}, \quad m = 1, 3, 5, \dots \tag{21}$$

$$\eta_n^s = \frac{n\pi}{2h}, \quad n = 0, 2, 4, 6, \dots \tag{22}$$

### 3.2. Dynamic Equilibrium Equations

For the numeric example, Equations (10a)-(10c) can be rewritten as

$$\begin{aligned} & C_{1111}u_{1,11} + C_{1122}u_{2,21} + C_{1133}u_{3,31} + \frac{1}{2}C_{1212}(u_{2,12} + u_{1,22}) \\ & + \frac{1}{2}C_{3131}(u_{3,13} + u_{1,33}) - e_{111}\varphi_{,11} - e_{311}\varphi_{,31} - q_{311}\psi_{,31} - q_{111}\psi_{,11} = \rho\ddot{u}_1 \end{aligned} \tag{23}$$

$$\begin{aligned} & C_{2211}u_{1,12} + C_{2222}u_{2,22} + C_{2233}u_{3,32} + \frac{1}{2}C_{2121}(u_{2,11} + u_{1,21}) \\ & + \frac{1}{2}C_{2323}(u_{2,33} + u_{3,23}) - e_{222}\varphi_{,22} - e_{223}\varphi_{,23} - q_{222}\psi_{,22} - q_{223}\psi_{,23} = \rho\ddot{u}_2 \end{aligned} \tag{24}$$

**Table 1.** Elastic parameters, unit (GPa).

$C_{1111} = C_{2222}$	$C_{1122} = C_{1133}$	$C_{2211} = C_{2233}$	$C_{3311} = C_{3322}$	$C_{3333}$	$C_{1212} = C_{2121}$	$C_{2323} = C_{3131}$
79.7	35.8	35.8	35.8	66.8	17.2	14.4

**Table 2.** Piezoelectric parameters, unit (C/m<sup>2</sup>); Piezomagnetic parameters, unit (Vs/m<sup>2</sup>).

Piezoelectric parameters, unit (C/m <sup>2</sup> )			Piezomagnetic parameters, unit (Vs/m <sup>2</sup> )		
$e_{111} = e_{222}$	$e_{333}$	$e_{232} = e_{311}$	$q_{111} = q_{222}$	$q_{333}$	$q_{232} = q_{311}$
-5.9	15.2	10.5	-60.9	156.8	108.3

**Table 3.** Dielectric parameters, unit (As/Am); Magnetic permeability parameters, unit (Vs/Am).

Dielectric parameters, unit (As/Am)			Magnetic permeability parameters, unit (Vs/Am)		
$\mathcal{G}_{111}$	$\mathcal{G}_{222}$	$\mathcal{G}_{333}$	$\mu_{111}$	$\mu_{222}$	$\mu_{333}$
$3.8 \times 10^{-10}$	$3.8 \times 10^{-10}$	$3.8 \times 10^{-10}$	$5.4 \times 10^{-6}$	$5.4 \times 10^{-6}$	$5.4 \times 10^{-6}$

$$C_{3311}u_{1,13} + C_{3322}u_{2,23} + C_{3333}u_{3,33} + \frac{1}{2}C_{3131}(u_{3,11} + u_{1,31}) + \frac{1}{2}C_{3232}(u_{3,22} + u_{2,32}) - e_{333}\varphi_{,33} - e_{232}\varphi_{,23} - e_{311}\varphi_{,13} - q_{333}\psi_{,33} - q_{232}\psi_{,23} - q_{311}\psi_{,13} = \rho\ddot{u}_3 \quad (25)$$

$$\frac{1}{2}e_{311}(u_{3,11} + u_{1,31}) + \frac{1}{2}e_{232}(u_{2,32} + u_{3,22}) + e_{111}u_{1,13} + e_{222}u_{2,23} + e_{333}u_{3,33} + g_{111}\varphi_{,11} + g_{222}\varphi_{,22} + g_{333}\varphi_{,33} = 0 \quad (26)$$

$$\frac{1}{2}q_{311}(u_{3,11} + u_{1,31}) + \frac{1}{2}q_{232}(u_{2,32} + u_{3,22}) + q_{111}u_{1,13} + q_{222}u_{2,23} + q_{333}u_{3,33} + \mu_{111}\psi_{,11} + \mu_{222}\psi_{,22} + \mu_{333}\psi_{,33} = 0 \quad (27)$$

Substituting of Equations (12), (17) and (18) into Equations (23)-(27), gives

$$-C_{1111}k_1^2u_1 - C_{1122}k_1k_2u_2 + C_{1133}ik_1u_{3,3} - \frac{1}{2}C_{1212}(k_1^2u_2 + k_1k_2u_1) - \frac{1}{2}C_{3131}(k_1^2u_3 - ik_1u_{1,3}) - e_{111}ik_1\varphi_{,3} + e_{311}k_1^2\varphi + q_{311}k_1^2\psi - q_{111}ik_1\psi_{,3} = -\rho\omega^2u_1 \quad (28)$$

$$-C_{2211}k_1k_2u_1 - C_{2222}k_2^2u_2 + C_{2233}ik_2u_{3,3} - \frac{1}{2}C_{2121}(k_1k_2u_2 + k_2^2u_1) - \frac{1}{2}C_{2323}(-ik_2u_{2,3} + k_2^2u_3) - e_{222}ik_2\varphi_{,3} + e_{232}k_2^2\varphi + q_{232}k_2^2\psi - q_{222}ik_2\psi_{,3} = -\omega^2\rho u_2 \quad (29)$$

$$C_{3311}ik_1u_{1,3} + C_{3322}ik_2u_{2,3} + C_{3333}u_{3,33} + \frac{1}{2}C_{3131}(ik_1u_{3,3} + u_{1,33}) + \frac{1}{2}C_{2323}(ik_2u_{3,3} + u_{2,33}) - e_{333}\varphi_{,33} - e_{232}ik_2\varphi_{,3} - e_{311}ik_1\varphi_{,3} - q_{333}\psi_{,33} - q_{232}ik_2\psi_{,3} - q_{311}ik_1\psi_{,3} = -\rho\omega^2u_3 \quad (30)$$

$$-\frac{1}{2}e_{311}(k_1^2u_3 - ik_1u_{1,3}) - \frac{1}{2}e_{232}(-ik_2u_{2,3} + k_2^2u_3) + e_{111}ik_1u_{1,3} + e_{222}ik_2u_{2,3} + e_{333}u_{3,33} - g_{111}k_1^2\varphi - g_{222}k_2^2\varphi + g_{333}\varphi_{,33} = 0 \quad (31)$$

$$-\frac{1}{2}q_{311}(k_1^2u_3 - ik_1u_{1,3}) - \frac{1}{2}q_{232}(-ik_2u_{2,3} + k_2^2u_3) + q_{111}ik_1u_{1,3} + q_{222}ik_2u_{2,3} + q_{333}u_{3,33} - \mu_{111}k_1^2\psi - \mu_{222}k_2^2\psi + \mu_{333}\psi_{,33} = 0 \quad (32)$$

The following equations can be obtained by using the orthogonality of the trigonometric function for Equations (28)-(32) and by dealing with the real and imaginary parts of Equations (28)-(32).

$$C_{3131}A_m \cos \frac{m\pi x_3}{2h} = e_{311}A_m^\varphi \cos \frac{m\pi x_3}{2h} + q_{311}A_m^\psi \cos \frac{m\pi x_3}{2h} \quad (33)$$

$$C_{2323}A_m \cos \frac{m\pi x_3}{2h} = e_{232}A_m^\varphi \cos \frac{m\pi x_3}{2h} + q_{232}A_m^\psi \cos \frac{m\pi x_3}{2h} \quad (34)$$

$$(C_{3131}k_1 + C_{2323}k_2)A_m \cos \frac{m\pi x_3}{2h} = e_{311}k_1A_m^\varphi \cos \frac{m\pi x_3}{2h} + q_{311}k_1A_m^\psi \cos \frac{m\pi x_3}{2h} \quad (35)$$

$$\left[ (e_{311} + e_{111})k_1^2 + (e_{232} + e_{222})k_2^2 + e_{333}(\eta_m^d)^2 \right] A_m \cos \frac{m\pi x_3}{2h} = - \left[ g_{111}k_1^2 + g_{222}k_2^2 + g_{333}(\eta_m^d)^2 \right] A_m^\varphi \cos \frac{m\pi x_3}{2h} \quad (36)$$

$$\begin{aligned} & \left[ (q_{311} + q_{111})k_1^2 + (q_{232} + q_{222})k_2^2 + e_{333}(\eta_m^d)^2 \right] A_m \cos \frac{m\pi x_3}{2h} \\ & = - \left[ \mu_{111}k_1^2 + \mu_{222}k_2^2 + \mu_{333}(\eta_m^d)^2 \right] A_m^\psi \cos \frac{m\pi x_3}{2h} \end{aligned} \quad (37)$$

$$\begin{aligned} & \left( -C_{1111}k_1^2 - C_{1122}k_2^2 - C_{1133}(\eta_m^d)^2 - C_{1212}k_1k_2 \right) A_m + e_{111}(\eta_m^d)^2 A_m^\phi \\ & + q_{111}(\eta_m^d)^2 A_m^\psi = -\rho\omega^2 A_m \end{aligned} \quad (38)$$

$$\begin{aligned} & \left( -C_{2211}k_1^2 - C_{2222}k_2^2 - C_{2233}(\eta_m^d)^2 - C_{2121}k_1k_2 \right) A_m + e_{222}(\eta_m^d)^2 A_m^\phi \\ & + q_{222}(\eta_m^d)^2 A_m^\psi = -\rho\omega^2 A_m \end{aligned} \quad (39)$$

$$\begin{aligned} & \left( -C_{3311}k_1^2 - C_{3322}k_2^2 - C_{3333}(\eta_m^d)^2 \right) A_m + e_{333}(\eta_m^d)^2 A_m^\phi \\ & + q_{333}(\eta_m^d)^2 A_m^\psi = -\rho\omega^2 A_m \end{aligned} \quad (40)$$

$$a_{11}F_{1n} + a_{12}F_{2n} + a_{13}F_{3n} + a_{14}F_{1n}^\phi + a_{15}F_{2n}^\phi + a_{16}F_{1n}^\psi + a_{17}F_{2n}^\psi = 0 \quad (41)$$

$$a_{21}F_{1n} + a_{22}F_{2n} + a_{23}F_{3n} + a_{24}F_{1n}^\phi + a_{25}F_{2n}^\phi + a_{26}F_{1n}^\psi + a_{27}F_{2n}^\psi = 0 \quad (42)$$

$$a_{31}F_{1n} + a_{32}F_{2n} + a_{33}F_{3n} + a_{34}F_{1n}^\phi + a_{35}F_{2n}^\phi + a_{36}F_{1n}^\psi + a_{37}F_{2n}^\psi = 0 \quad (43)$$

$$a_{41}F_{1n} + a_{42}F_{2n} + a_{43}F_{3n} + a_{44}F_{1n}^\phi + a_{45}F_{2n}^\phi + a_{46}F_{1n}^\psi + a_{47}F_{2n}^\psi = 0 \quad (44)$$

$$a_{51}F_{1n} + a_{52}F_{2n} + a_{53}F_{3n} + a_{54}F_{1n}^\phi + a_{55}F_{2n}^\phi + a_{56}F_{1n}^\psi + a_{57}F_{2n}^\psi = 0 \quad (45)$$

$$a_{61}F_{1n} + a_{62}F_{2n} + a_{63}F_{3n} + a_{64}F_{1n}^\phi + a_{65}F_{2n}^\phi + a_{66}F_{1n}^\psi + a_{67}F_{2n}^\psi = 0 \quad (46)$$

$$a_{71}F_{1n} + a_{72}F_{2n} + a_{73}F_{3n} + a_{74}F_{1n}^\phi + a_{75}F_{2n}^\phi + a_{76}F_{1n}^\psi + a_{77}F_{2n}^\psi = 0 \quad (47)$$

$$\begin{aligned} & a_{81}F_{1n}(\eta_n^s)\cos(\eta_n^s x_3) + a_{82}F_{2n}(\eta_n^s)\cos(\eta_n^s x_3) + a_{83}F_{3n}(\eta_n^s)\cos(\eta_n^s x_3) \\ & + a_{84}F_{1n}^\phi(\eta_m^s)\cos(\eta_m^s x_3) + a_{85}F_{2n}^\phi(\eta_m^s)\cos(\eta_m^s x_3) \\ & + a_{86}F_{1n}^\psi(\eta_n^s)\cos(\eta_n^s x_3) + a_{87}F_{2n}^\psi(\eta_n^s)\cos(\eta_n^s x_3) = 0 \end{aligned} \quad (48)$$

The above Equations (32)-(40) do not contain the shear term  $\eta_n^s$ , so they are P-wave equations. Equations (41)-(48) are not related to the dilatation wave term  $\eta_m^d$ , so they are S-wave equations. This indicates that the kind of wave is invariable after reflection. Equations (33)-(37) and Equations (48) are true according to Saint-Venant's principle.  $a_{ij}$  in Equations (41)-(48) are given by **Appendix A**.

#### 4. Wave Characteristics

Equations (38)-(40) about the longitudinal wave can be written in the following matrix form

$$\begin{bmatrix} b_{11} - \rho\omega^2 & -b_{12} & -b_{13} \\ b_{21} - \rho\omega^2 & -b_{22} & -b_{23} \\ b_{31} - \rho\omega^2 & -b_{32} & -b_{33} \end{bmatrix} \begin{Bmatrix} A_m \\ A_m^\phi \\ A_m^\psi \end{Bmatrix} = \begin{Bmatrix} 0 \\ 0 \\ 0 \end{Bmatrix} \quad (49)$$

For Equation (49) to have a nontrivial solution, it is required that

$$\begin{vmatrix} b_{11} - \rho\omega^2 & -b_{12} & -b_{13} \\ b_{21} - \rho\omega^2 & -b_{22} & -b_{23} \\ b_{31} - \rho\omega^2 & -b_{32} & -b_{33} \end{vmatrix} = 0 \tag{50}$$

where  $b_{ij} (i, j = 1, 2, 3)$  are given by **Appendix B**.

The relationship of wave number  $p = \sqrt{k^2 + m^2}$  and circle frequencies  $\omega$  can be obtained by solving Equation (50), and then phase velocity is defined as

$$c = \frac{\omega}{p} \tag{51}$$

and phase velocity surface

$$f = c(\theta, \omega, p) = 0 \tag{52}$$

can be obtained.

Before plotting the figures, we introduce the dimensionless frequency  $\bar{\omega} = \omega/c_p$ , phase wave velocity  $\bar{c} = c/c_p$ , where  $c_p = \sqrt{c_{1111}/\rho}$ .

**Figure 2** shows the dispersion spectrum of the electric-magneto-elastic plate (EMEP) about longitudinal waves with  $m = 1, 7, 13$  and  $19$ . The dispersion curves affected by the geometric boundaries and material properties are compared in detail in **Figures 2(a)-(c)**. The four Figures are, respectively, the phase

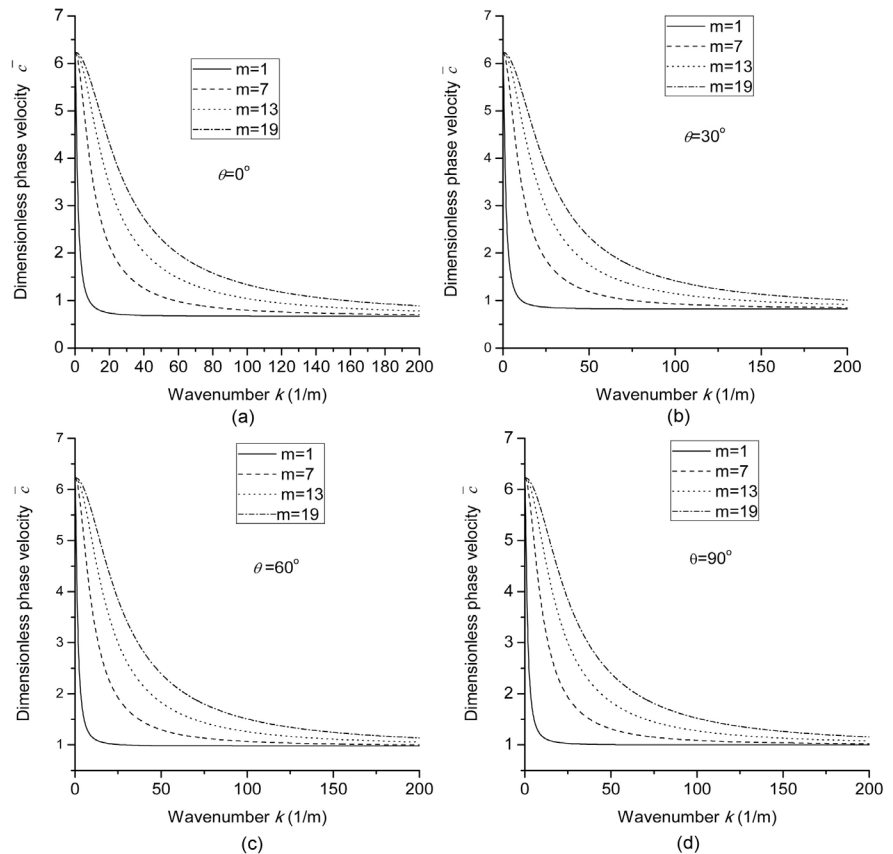


**Figure 2.** Dimensionless phase velocity curves of dilatation wave in the electric-magneto-elastic plate when the incident angle  $\theta$  is  $0^\circ$  (a),  $\theta$  is  $30^\circ$  (b),  $\theta$  is  $60^\circ$  (c) and  $\theta$  is  $90^\circ$  (d).

velocity curves in the different incident direction  $\theta$ . It can be found from the four Figures that with the increase of  $m$ , the dispersion of wave becomes more and more serious. The larger  $m$  is, the closer the direction of wave propagation is to the thickness of the plate, this means that the closer the wave propagation direction is to the direction  $x_3$ , the more dispersive it is. This can be explained as that the geometrical and material dispersion of longitudinal wave propagating along the thickness direction is more serious than propagating in middle plane.

**Figure 3** shows the phase velocity surfaces of EMEP about longitudinal waves with the wave number  $m = 3$  and  $k = 2, 20, 200$ . These left graphs and the right ones are drawn in the absolute and relative coordinate systems, respectively. It

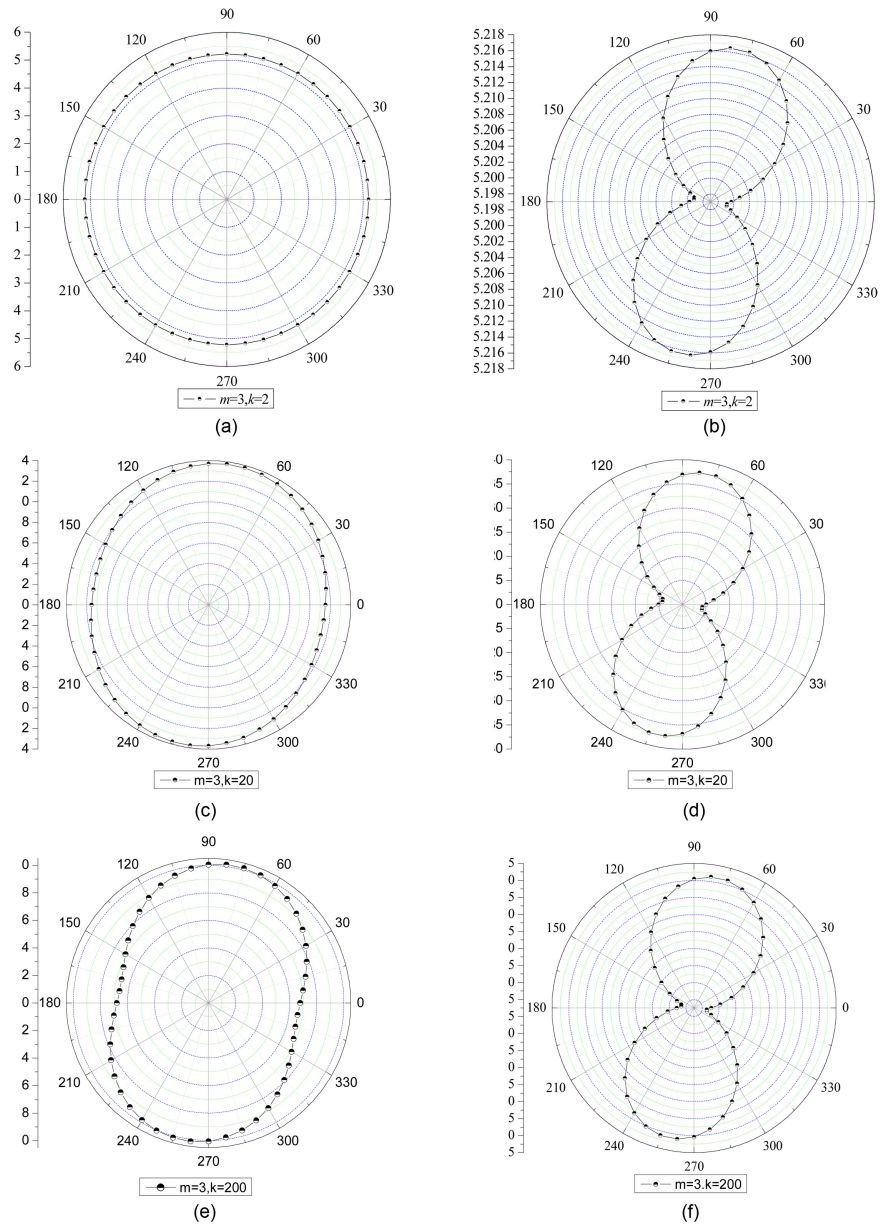


**Figure 3.** Phase velocity surface of longitudinal wave in the electric-magneto-elastic plate when  $m = 3, k = 2, 20, 200$ .

can be seen from comparison of the left Figures of **Figures 3(a)-(c)** that the phase velocity surface changes from an approximate circular to an approximate ellipse as the wave number  $k$  changes from 2 to 200. This is due to the anisotropy in the  $x_1 0x_2$  plane caused by the polarization of the electromagnetic field along the  $x_3$ -axis. It can be found from right Figures of **Figure 3** that the phase velocity surfaces are symmetrical about  $\theta = 75^\circ$  and  $\theta = 165^\circ$ , this means that EMEP is approximately orthotropic.

To further clarify the conclusions obtained from **Figure 3**. Without loss of generality, **Figure 4** is drawn when the representative wave numbers  $m = 51$  and  $k = 20, 200, 2000$  are taken. The same conclusions can be obtained from **Figure 4** as these from **Figure 3**.

The matrix form of Equations (41)-(47) about the shear wave can be written as

$$\begin{bmatrix} a_{11} & a_{12} & a_{13} & a_{14} & a_{15} & a_{16} & a_{17} \\ a_{21} & a_{22} & a_{23} & a_{24} & a_{25} & a_{26} & a_{27} \\ a_{31} & a_{32} & a_{33} & a_{34} & a_{35} & a_{36} & a_{37} \\ a_{41} & a_{42} & a_{43} & a_{44} & a_{45} & a_{46} & a_{47} \\ a_{51} & a_{52} & a_{53} & a_{54} & a_{55} & a_{56} & a_{57} \\ a_{61} & a_{62} & a_{63} & a_{64} & a_{65} & a_{66} & a_{67} \\ a_{71} & a_{72} & a_{73} & a_{74} & a_{75} & a_{76} & a_{77} \end{bmatrix} \begin{Bmatrix} F_{1n} \\ F_{2n} \\ F_{3n} \\ F_{1n}^\phi \\ F_{2n}^\phi \\ F_{1n}^\psi \\ F_{2n}^\psi \end{Bmatrix} = \begin{Bmatrix} 0 \\ 0 \\ 0 \\ 0 \\ 0 \\ 0 \\ 0 \end{Bmatrix} \quad (53)$$

The condition of the nontrivial solution of Equation (53) is that the coefficient determinant of Equation (53) must be zero.

$$\begin{vmatrix} a_{11} & a_{12} & a_{13} & a_{14} & a_{15} & a_{16} & a_{17} \\ a_{21} & a_{22} & a_{23} & a_{24} & a_{25} & a_{26} & a_{27} \\ a_{31} & a_{32} & a_{33} & a_{34} & a_{35} & a_{36} & a_{37} \\ a_{41} & a_{42} & a_{43} & a_{44} & a_{45} & a_{46} & a_{47} \\ a_{51} & a_{52} & a_{53} & a_{54} & a_{55} & a_{56} & a_{57} \\ a_{61} & a_{62} & a_{63} & a_{64} & a_{65} & a_{66} & a_{67} \\ a_{71} & a_{72} & a_{73} & a_{74} & a_{75} & a_{76} & a_{77} \end{vmatrix} = 0 \quad (54)$$

Before plotting the Figures, we introduce the dimensionless frequency  $\bar{\omega} = \omega/c_s$ , the phase wave velocity  $\bar{c} = c/c_s$  and the group velocity  $C_g = c_g/c_s$ , where  $c_s = \sqrt{c_{1313}/\rho}$ . The symbols of EMEP and EP denote the electric-magnetic-elastic plate and the elastic plate, respectively.

In the subsequent example, let  $n = 2$ ,  $\theta = 0^\circ, 30^\circ, 60^\circ$  and  $90^\circ$  in Equations (54) and (56). The dimensionless circle frequency and the phase velocity corresponding to the different wave numbers  $k$  can be obtained from the solution of Equation (54) and Equation (56), respectively. For the purpose of investigation to the effects of the piezoelectric and the piezomagnetic parameters on the dispersion characteristics of the shear waves, we consider the EMEP and the elastic plate EP with the same modulus of elasticity as the former. The dispersion curves of shear waves with the different incident angles  $\theta$ , namely, the relationship curves of the dimensionless circle frequency  $\omega$  and the wave number  $k$ , are

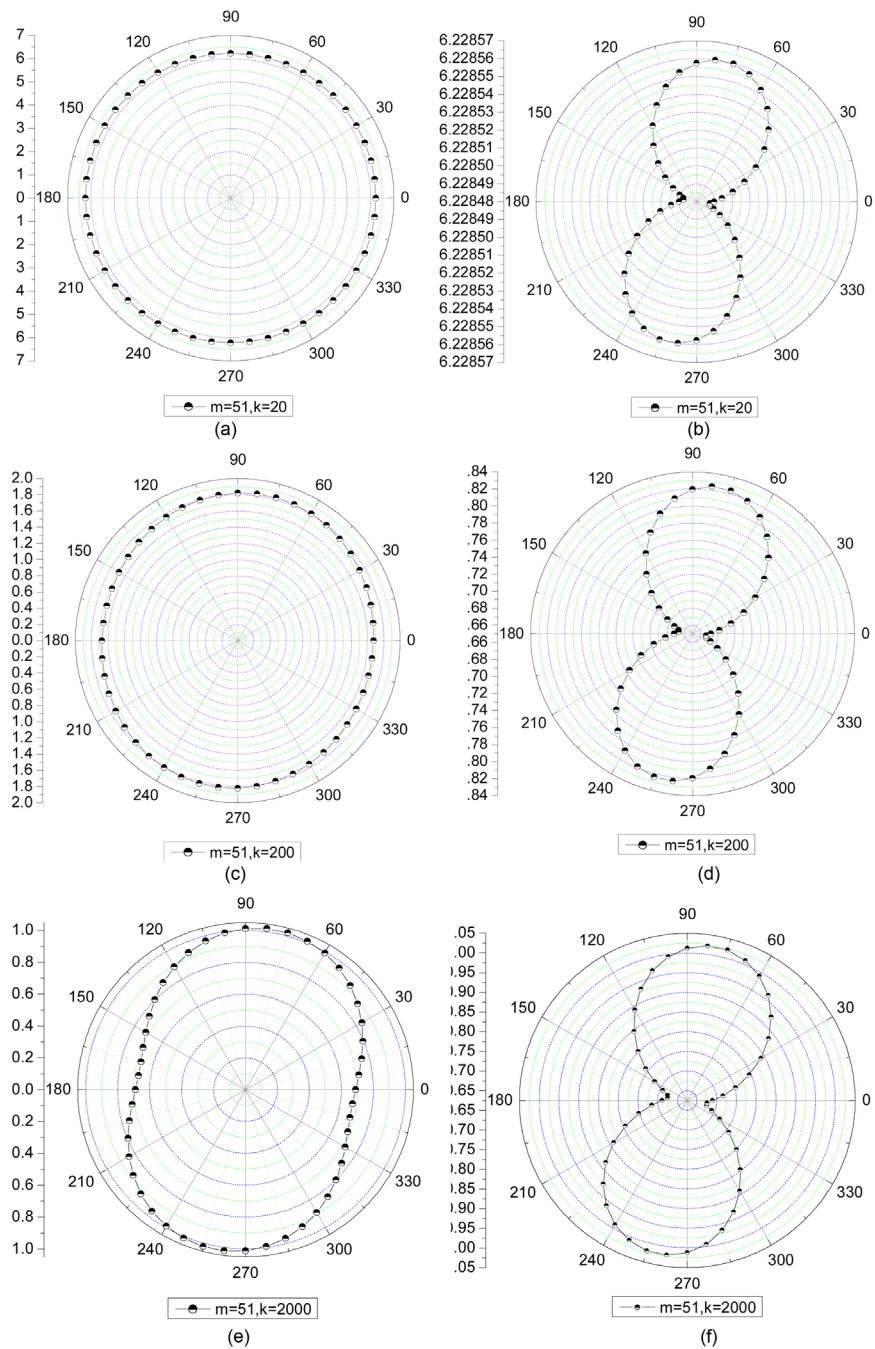


**Figure 4.** Phase velocity surface of longitudinal wave in the electric-magneto-elastic plate when  $m = 51$ ,  $k = 20, 200$  and  $2000$ .

plotted in **Figures 5(a)-8(a)**. The relationship curves of the dimensionless phase velocity  $C$  and the wave number  $k$  are plotted in **Figures 5(b)-8(b)**.

When the incident angle  $\theta$  is  $0^\circ$ , the relationship curves between the dimensionless circle frequencies and the wave numbers for EP and EMEP are shown in **Figure 5(a)**. The phase velocity dispersion curves corresponding to them are shown in **Figure 5(b)**. It can be seen from **Figure 5(a)** and **Figure 5(b)** that the shear waves in EP and EMEP are dispersive. As can be seen, the dispersion

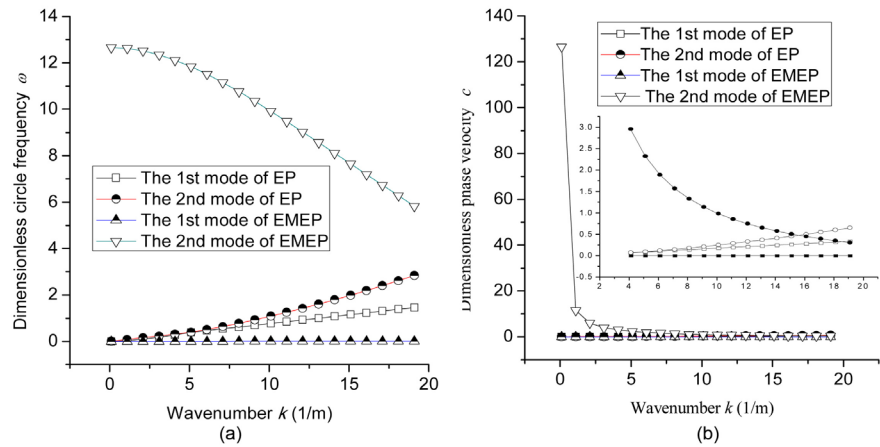


**Figure 5.** Dispersion curves of the different wave modes for EP and EME when  $\theta$  is  $0^\circ$ .

curves of waves in the two plates are different, especially that of the second wave mode. This indicates that the dispersion characteristics of wave are affected by the piezoelectric and piezomagnetic parameters. It also can be found from **Figure 5(b)** that effect of the piezoelectric and the piezomagnetic parameters on the phase velocities of the shear waves with the small wave number  $k$  is very obvious. The smaller  $k$  is, the closer the propagation direction of shear wave is to the thickness direction of the plate. This means that the dispersion of shear wave propagating along the thickness direction of the plate is more serious than that along the middle plane of the plate.

When  $\theta$  is  $30^\circ$ , the dispersion curves of the different wave modes for EP and EMEP are shown in **Figure 6**. It can be found from the comparison of **Figure 6(a)** with **Figure 5(a)** that the dispersion characteristics of the waves propagating along the direction  $\theta = 30^\circ$  is different from that along the direction  $\theta = 0^\circ$ , it is cause that EMEP is anisotropic. It can also be seen from **Figure 6(a)** that the piezoelectric and piezomagnetic parameters have a great influence on the dispersion characteristics of the various shear wave modes, and from **Figure 6(b)** that the piezoelectric and piezomagnetic parameters have a great influence on the phase velocity of shear waves with the small wave number  $k$ , especially that of the third wave mode.

When the incident angle  $\theta$  is  $60^\circ$ , the dispersion curves of the different wave modes for EP and EMEP are shown in **Figure 7**. It can be found from the comparisons of **Figure 7(a)** with both **Figure 5(a)** and **Figure 6(a)** that the dispersion curves in **Figure 7(a)** are different from these in **Figure 5(a)** and **Figure 6(a)**, it can be also seen from **Figure 7(a)** that piezoelectric and piezomagnetic parameters have a great influence on the dispersion characteristics of various shear wave modes, from **Figure 7(b)** that the piezoelectric and piezomagnetic parameters have a great influence on the phase velocity of the shear waves with the small wave number  $k$ , especially that of the third wave mode.

When the incident angle  $\theta$  is  $90^\circ$ , the dispersion curves of the different shear wave modes for EP and EMEP are shown in **Figure 8**. The shear wave propagating along the incident angle  $90^\circ$  is in reality 2-D wave. It can be found from

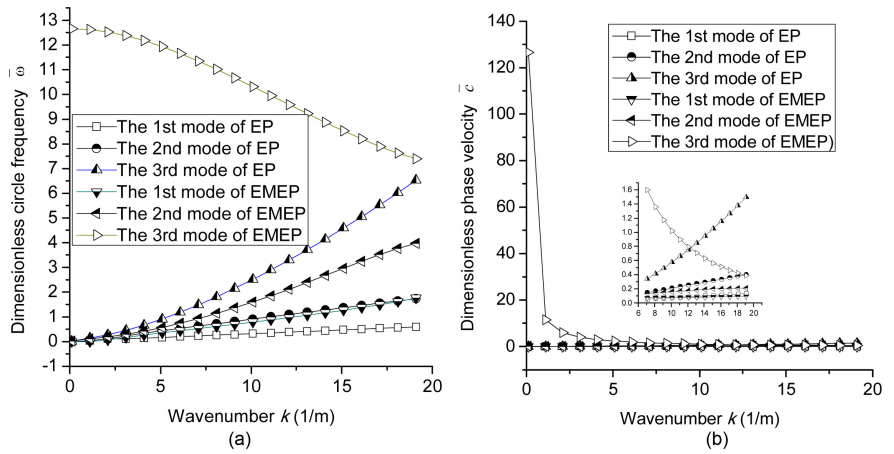


**Figure 6.** Dispersion curves of the different wave modes for the EP and the EMEP when  $\theta$  is  $30^\circ$ .

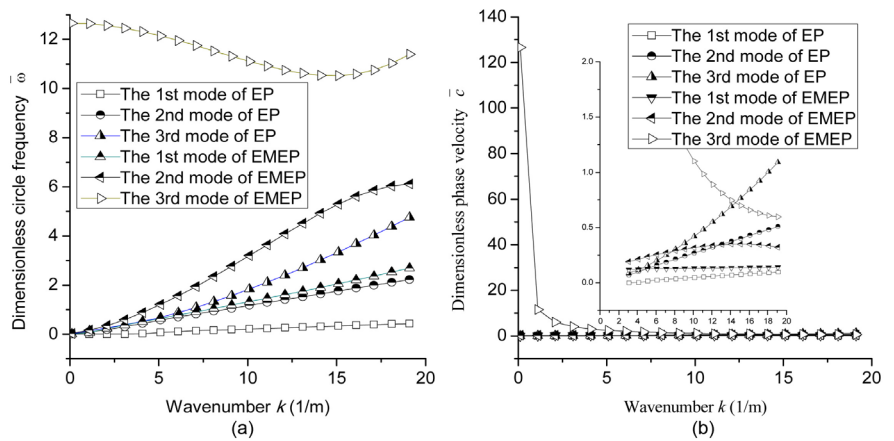


**Figure 7.** Dispersion curves of the different wave modes for EP and EMEP when  $\theta$  is  $60^\circ$ .

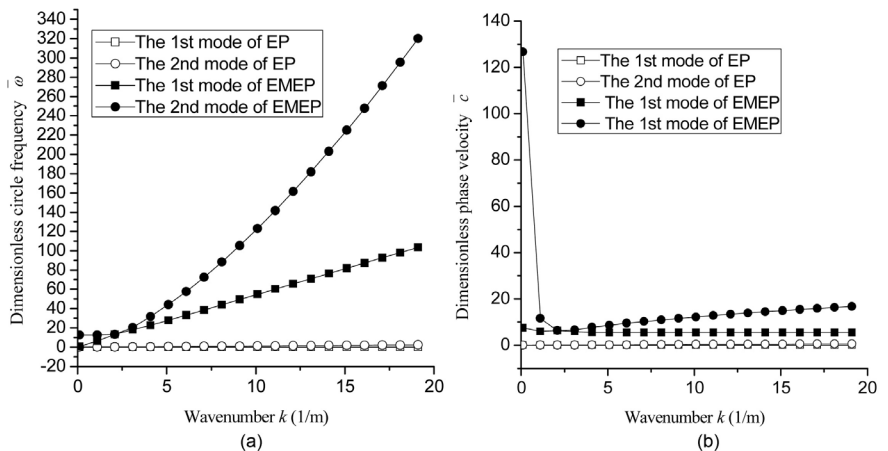


**Figure 8.** Dispersion curves of the different wave modes for EP and EMEP when  $\theta$  is  $90^\circ$ .

**Figure 8(a)** that the piezoelectric and piezomagnetic parameters have a great influence on the dispersion characteristics of the various shear wave modes, and from **Figure 8(b)** that the piezoelectric and piezomagnetic parameters have a

great influence on the phase velocity of the shear waves with the small wave number  $k$ , especially that of the second wave mode.

The phase velocity surface of the third shear wave mode for EMEP is shown in **Figure 9** when the wave number  $n = 2$  and  $k = 2, 20$  and  $40$ . **Figure 9(a)**, **Figure 9(c)**, **Figure 9(e)** are drawn in the absolute coordinate, **Figure 9(b)**, **Figure 9(d)**, **Figure 9(f)** are drawn in the relative coordinate. By comparing **Figure 9(a)**, **Figure 9(c)**, **Figure 9(e)**, it can be seen that the phase velocity surface changes from an approximate circle to a non-circle as the wave number  $k$

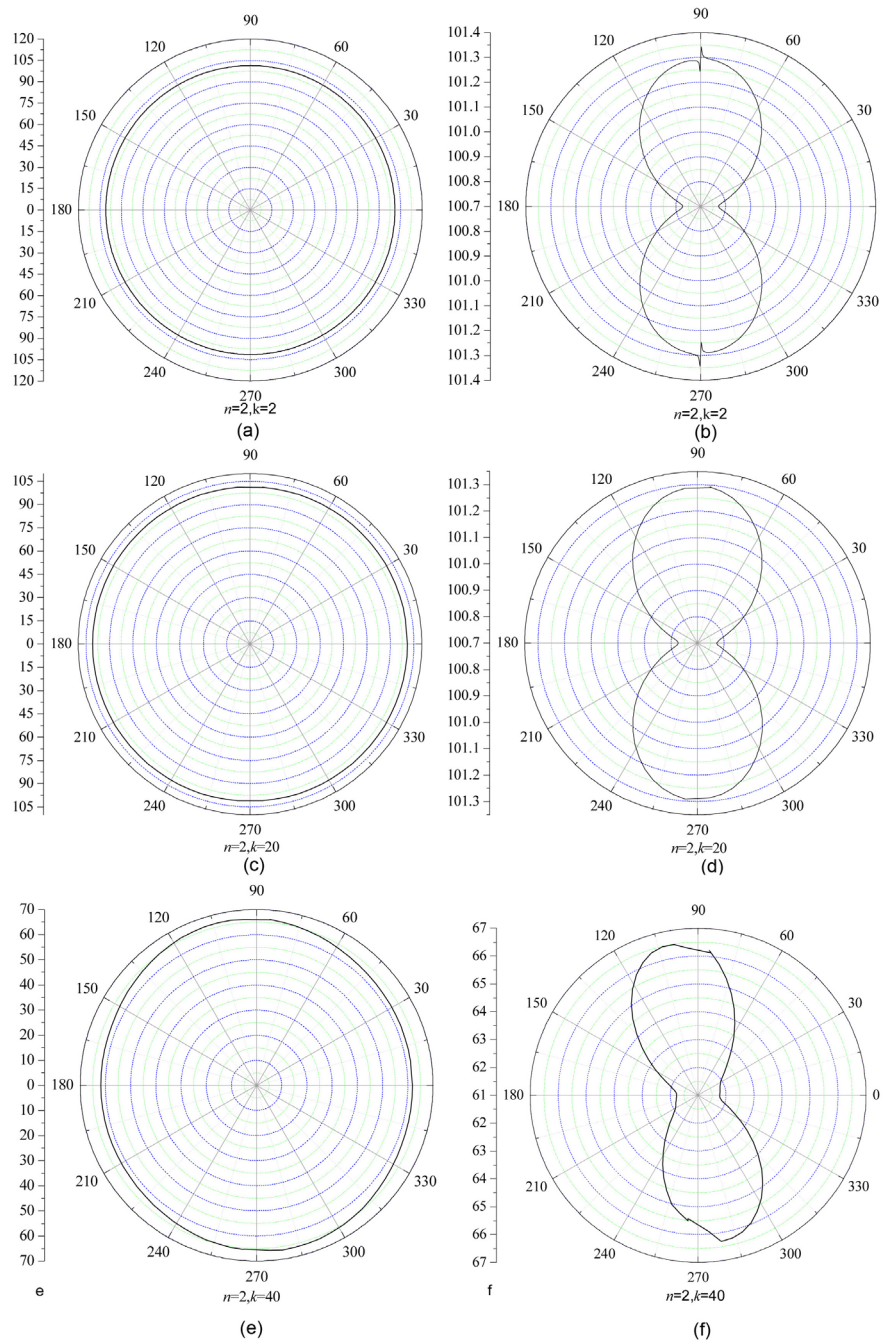


**Figure 9.** Phase velocity surface of shear wave in EMEP when  $n = 2$ ,  $k = 2, 20$  and  $40$ .

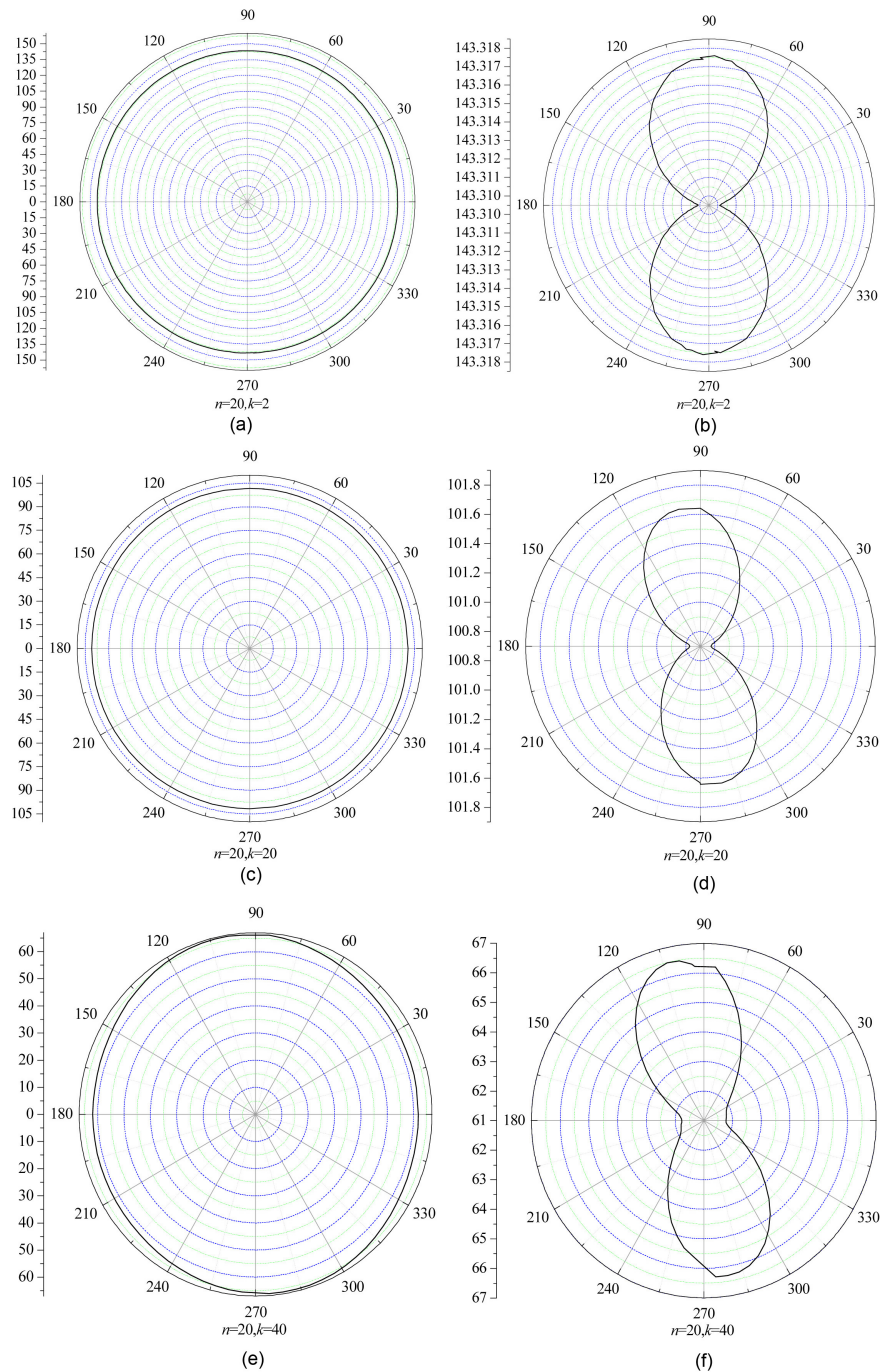


**Figure 10.** Phase velocity surface of shear wave in EMEP when  $n = 20$ ,  $k = 2$ , 20 and 40.

changes from 2 to 40, this means that the closer the direction of wave propagating is the middle plane  $x_1Ox_2$ , the more different the phase velocities of the wave propagating along the different directions are. It can be found from comparison of **Figure 9(b)**, **Figure 9(d)**, **Figure 9(f)** that the phase velocity surface rotates counter clockwise with the change of wave number  $k$  from 2 to 40, and the phase velocity plane is anti-symmetry about coordinate origin.

To further clarify the conclusions obtained from **Figure 9**, **Figure 10** is drawn

when the representative wave number  $n = 20$  and  $k = 2, 20$  and  $40$ . The same conclusions can be obtained from **Figure 10** as that from **Figure 9**.

## 5. Conclusions

The bulk wave in the electromagnetic elastic plate is studied, and the following conclusions are obtained by the numerical examples:

- 1) The types of P-wave and S-wave reflected by the boundary of the plate remain unchanged.
- 2) The dispersion of the wave propagating along the mid-plane is less than that of the wave propagating along the plate thickness.
- 3) The closer the propagating direction of the longitudinal and the shear waves are to the middle plane, the more different their phase velocities in different directions are.
- 4) The phase velocity surface of the shear wave is anti-symmetry about the coordinate origin.
- 5) The phase velocity surface of a longitudinal wave is symmetrical about  $\theta = 75^\circ$  and  $\theta = 165^\circ$ , this means that EMEP is approximately orthotropic.

## Acknowledgements

This work is supported by National Natural Science Foundation of China under the Grant Number 11372109.

## Conflicts of Interest

The authors declare no conflicts of interest regarding the publication of this paper.

## References

- [1] Harse, G., Dougherty, J.P. and Newnham, R.E. (1993) Theoretical Modelling of 3-0/0-3 Magnetolectric Composites. *International Journal of Applied Electromagnetics in Materials*, **4**, 161-171.
- [2] Avellaneda, M. and Harse, G. (1994) Magnetolectric Effect in Piezoelectric Magnetostrictive (2-2) Composites. *Journal of Intelligent Material Systems and Structure*, **5**, 501-513. <https://doi.org/10.1177/1045389X9400500406>
- [3] Cupiał, P. (2015) Three-Dimensional Perturbation Solution of the Natural Vibrations of Piezoelectric Rectangular Plates. *Journal of Sound and Vibration*, **351**, 143-160. <https://doi.org/10.1016/j.jsv.2015.04.006>
- [4] Nie, G.Q., Liu, J.X., Fang, X.Q. and An, Z.J. (2012) Shear Horizontal (SH) Waves Propagating in Piezo-Electric-Piezomagnetic Bilayer System with an Imperfect Interface. *Acta Mechanica*, **223**, 1999-2009. <https://doi.org/10.1007/s00707-012-0680-6>
- [5] Ezzin, H., Amor, M.B. and Ghozlen, M.H.B. (2017) Lamb Waves Propagation in Layered Piezoelectric/Piezomagnetic Plates. *Ultrasonics*, **76**, 63-69. <https://doi.org/10.1016/j.ultras.2016.12.016>
- [6] Guo, X., Wei, P.J., Li, L. and Lan, M. (2018) Effects of Functionally Graded Interlayers on Dispersion Relations of Shear Horizontal Waves in Layered Piezoelec-

- tric/Piezomagnetic Cylinders. *Applied Mathematical Modelling*, **55**, 569-582.  
<https://doi.org/10.1016/j.apm.2017.11.029>
- [7] Yu, J.G., Lefebvre, J.E. and Zhang Ch. (2014) Guided Wave in Multilayered Piezoelectric-Piezomagnetic Bars with Rectangular Cross-Sections. *Composite Structures*, **116**, 336-345. <https://doi.org/10.1016/j.compstruct.2014.04.025>
- [8] Pang, Y., Liu, Y.S., Liu, J.X., *et al.* (2016) Propagation of SH Waves in an Infinite/Semi-Infinite Piezoelectric/Piezomagnetic Periodically Layered Structure. *Ultrasonics*, **67**, 120-128. <https://doi.org/10.1016/j.ultras.2016.01.007>
- [9] Wang, Y.Z., Li, F.M., Huang, W.H., *et al.* (2008) Wave Band Gaps in Two-Dimensional Piezoelectric/Piezomagnetic Phononic Crystals. *International Journal of Solids and Structures*, **45**, 4203-4210.  
<https://doi.org/10.1016/j.ijsolstr.2008.03.001>
- [10] Li, L. and Wei, P.J. (2014) The Piezoelectric and Piezomagnetic Effect on the Surface Wave Velocity of Magneto-Electro-Elastic Solids. *Journal of Sound and Vibration*, **333**, 2312-2326. <https://doi.org/10.1016/j.jsv.2013.12.005>
- [11] Pang, Y., Wang, Y.S., Liu, J.X. and Fang, D.N. (2008) Reflection and Refraction of Plane Waves at the Interface Between Piezoelectric and Piezomagnetic Media. *International Journal of Engineering Science*, **46**, 1098-1110.  
<https://doi.org/10.1016/j.ijengsci.2008.04.006>
- [12] Arfi, M. (2016) Analysis of Wave in a Functionally Graded Magneto-Electro-Elastic Nano-Rod Using Nonlocal Elasticity Model Subjected to Electric and Magnetic Potentials. *Acta Mechanica*, **227**, 2529-2542.  
<https://doi.org/10.1007/s00707-016-1584-7>

## Appendix A

$$\begin{aligned}
 a_{11} &= (C_{1122} - C_{1133})k_1k_2 + 0.5C_{1212}k_1^2, \\
 a_{12} &= (-C_{1111} + C_{1133})k_1^2 - 0.5C_{1212}k_1k_2 - \rho\omega^2 \\
 a_{13} &= -0.5C_{3131}k_1k_2, \\
 a_{14} &= -e_{111}k_1k_2, \\
 a_{15} &= e_{111}k_1^2, \\
 a_{16} &= -q_{111}k_1k_2, \\
 a_{17} &= q_{111}k_1^2 \\
 a_{21} &= -0.5C_{3131}k_1^2k_2, \\
 a_{22} &= 0.5C_{3131}k_1^3 - 0.5C_{3131}k_1(\eta_m^s)^2, \\
 a_{23} &= (C_{1111} + C_{1122})k_1^2k_2 + 0.5C_{1212}k_1^3 + 0.5C_{1212}k_1k_2^2 - \rho\omega^2k_2, \\
 a_{24} &= e_{311}k_1^2k_2, \\
 a_{25} &= -e_{311}k_1^3 \\
 a_{26} &= q_{311}k_1^2k_2, \\
 a_{27} &= -q_{311}k_1^3, \\
 a_{31} &= (C_{2222} - C_{2233})k_2^2 - 0.5C_{2121}k_1k_2 - \rho\omega^2 \\
 a_{32} &= (-C_{2211} + C_{2233})k_1k_2 - 0.5C_{2121}k_2^2, \\
 a_{33} &= -0.5C_{2323}k_1k_2, \\
 a_{34} &= e_{222}k_2^2, \\
 a_{35} &= -e_{222}k_1k_2, \\
 a_{36} &= q_{222}k_2^2, \\
 a_{37} &= -q_{222}k_1k_2, \\
 a_{41} &= -0.5C_{2323}k_2^3 + 0.5C_{2323}k_2(\eta_m^s)^2, \\
 a_{42} &= 0.5C_{2323}k_1k_2^2, \\
 a_{43} &= (C_{2211} - C_{2222})k_1k_2^2 + 0.5C_{2121}(k_2k_1^2 + k_2^3) - \rho\omega^2k_1, \\
 a_{44} &= e_{232}k_2^3, \\
 a_{45} &= -e_{232}k_1k_2^2 \\
 a_{46} &= q_{232}k_2^3, \\
 a_{47} &= -q_{232}k_1k_2^2, \\
 a_{51} &= (C_{3322} + C_{3333})k_2(\eta_m^s)^2 - \rho\omega^2k_2, \\
 a_{52} &= (C_{3311} - C_{3333})k_1(\eta_m^s)^2 + \rho\omega^2k_1, \\
 a_{53} &= 0.5(C_{3131}k_2 - C_{2323}k_1)(\eta_m^s)^2, \\
 a_{54} &= e_{333}k_2(\eta_m^s)^2, \\
 a_{55} &= -e_{333}k_1(\eta_m^s)^2, \\
 a_{56} &= q_{333}k_2(\eta_m^s)^2, \\
 a_{57} &= -q_{333}k_1(\eta_m^s)^2, \\
 a_{61} &= 0.5e_{311}k_1^2k_2 + 0.5e_{232}k_2[k_2^2 + (\eta_m^s)^2] + (e_{222} + e_{333})k_2(\eta_m^s)^2, \\
 a_{62} &= 0.5e_{311}k_1[k_1^2 + (\eta_m^s)^2] - 0.5e_{232}k_1k_2^2 + (e_{111} - e_{333})k_1(\eta_m^s)^2, \\
 a_{63} &= 0, \\
 a_{64} &= g_{111}k_1^2k_2 + g_{222}k_2^3 + g_{333}k_2(\eta_m^s)^2,
 \end{aligned}$$

$$\begin{aligned}
a_{65} &= -g_{111}k_1^3 - g_{222}k_1k_2^2 - g_{333}k_1(\eta_m^s)^2, \\
a_{66} &= a_{67} = 0 \\
a_{71} &= 0.5q_{311}k_1^2k_2 + 0.5q_{232}k_2 \left[ k_2^2 + (\eta_m^s)^2 \right] + (q_{222} + q_{333})k_2(\eta_m^s)^2 \\
a_{72} &= 0.5q_{311}k_1 \left[ k_1^2 + (\eta_m^s)^2 \right] - 0.5q_{232}k_1k_2^2 + (q_{111} - q_{333})k_1(\eta_m^s)^2, \\
a_{73} &= a_{74} = a_{75} = 0, \\
a_{76} &= \mu_{111}k_1^2k_2 + \mu_{222}k_2^3 + \mu_{333}k_2(\eta_m^s)^2, \\
a_{77} &= -\mu_{111}k_1^3 - \mu_{222}k_1k_2^2 - \mu_{333}k_1(\eta_m^s)^2, \\
a_{81} &= 0.5C_{3131}k_1k_2 + 0.5C_{2323} \left[ k_2^2 - (\eta_m^s)^2 \right], \\
a_{82} &= -0.5C_{2323}k_1k_2 - 0.5C_{3131} \left[ k_1^2 - (\eta_m^s)^2 \right] \\
a_{83} &= -(C_{3311} + C_{3322})k_1k_2, \\
a_{84} &= -e_{311}k_1k_2, \\
a_{85} &= e_{311}k_1^2, \\
a_{86} &= -q_{311}k_1k_2, \\
a_{87} &= q_{311}k_1^2
\end{aligned}$$

## Appendix B

$$\begin{aligned}
b_{11} &= C_{1111}k_1^2 + C_{1122}k_2^2 + C_{1133}(\eta_m^d)^2 + C_{1212}k_1k_2 \\
b_{12} &= e_{111}(\eta_m^d)^2 \\
b_{13} &= q_{111}(\eta_m^d)^2 \\
b_{21} &= C_{2211}k_1^2 + C_{2222}k_2^2 + C_{2233}(\eta_m^d)^2 + C_{2121}k_1k_2 \\
b_{22} &= e_{222}(\eta_m^d)^2 \\
b_{23} &= q_{222}(\eta_m^d)^2 \\
b_{31} &= C_{3311}k_1^2 + C_{3322}k_2^2 + C_{3333}(\eta_m^d)^2 \\
b_{32} &= e_{333}(\eta_m^d)^2 \\
b_{33} &= q_{333}(\eta_m^d)^2
\end{aligned}$$